forests

MDPI

Article

Morphological Characteristics and Water-Use Efficiency of Siberian Elm Trees (*Ulmus pumila* L.) within Arid Regions of Northeast Asia

Go Eun Park [1], Don Koo Lee [2,†], Ki Woo Kim [3,†], Nyam-Osor Batkhuu [4,†], Jamsran Tsogtbaatar [5,†], Jiao-Jun Zhu [6,†], Yonghuan Jin [6,†], Pil Sun Park [2,†], Jung Oh Hyun [2,†] and Hyun Seok Kim [2,7,8,9,*]

1 Center for Forest and Climate Change, National Institute of Forest Science, Seoul 02455, Korea; goeunpark@korea.kr
2 Department of Forest Sciences, Seoul National University, Seoul 08826, Korea; dklee@snu.ac.kr (D.K.L.); pspark@snu.ac.kr (P.S.P.); junghyun@snu.ac.kr (J.O.H.)
3 School of Ecology and Environmental System, Kyungpook National University, Sangju 37224, Korea; kiwoo@knu.ac.kr
4 Department of Forestry, National University of Mongolia, Ulaanbaatar 210646, Mongolia; batkhuu@num.edu.mn
5 Institute of Geoecology, Mongolian Academy of Sciences, Ulaanbaatar 211238, Mongolia; geoeco@magicnet.mn
6 Institute of Applied Ecology, Chinese Academy of Sciences, Shenyang 110016, China; jiaojunzhu@iae.ac.cn (J.-J.Z.); jinyh@iae.ac.cn (Y.J.)
7 Institute of Future Environmental and Forest Resources, Research Institute for Agriculture and Life Sciences, Seoul National University, Seoul 08826, Korea
8 National Center for Agro Meteorology, Seoul 08826, Korea
9 Interdisciplinary Program in Agriculture and Forest Meteorology, Seoul National University, Seoul 08826, Korea
* Correspondence: cameroncrazies@snu.ac.kr; Tel.: +82-2-880-4752; Fax: +82-2-873-3560
† These authors contributed equally to this work.

Academic Editors: Jarmo K. Holopainen and Timothy A. Martin
Received: 31 August 2016; Accepted: 8 November 2016; Published: 17 November 2016

Abstract: The Siberian elm (*Ulmus pumila* L.) is one of the most commonly found tree species in arid areas of northeast Asia. To understand the morphological and physiological characteristics of Siberian elms in arid regions, we analyzed leaves from seven study sites (five arid or semi-arid and two mesic) in China, Mongolia and the Republic of Korea, which covered a wide range of average annual precipitation (232 mm·year^{-1} to 1304 mm·year^{-1}) under various aridity indexes (AI) and four different microenvironments: sand dune, steppe, riverside and forest. The traits of Siberian elms varied widely along different annual precipitation (P) and AI gradients. Tree height (H), leaf size (LS) and stomatal area per unit leaf area (A_S/A_L) decreased with increasing AI, whereas leaf mass per unit leaf area (LMA) and water-use efficiency (WUE) increased significantly. In addition, trees at the five arid sites showed significant differences in LS, LMA and A_S/A_L but not in H and WUE. Thus, our study indicated that indigenous Siberian elm trees in arid areas have substantially altered their morphological and physiological characteristics to avoid heat stress and increase water conservation in comparison to mesic areas. However, their changes differed depending on the surrounding microenvironment even in arid areas. Trees in sand dunes had a smaller LS, higher LMA, thicker leaf cuticle layer and higher stomatal density and A_S than those in steppes and near a riverside.

Keywords: drought tolerance; leaf size; leaf mass per area; microenvironment; stomatal density and area; water-use efficiency ($\delta^{13}C$)

1. Introduction

Drylands cover more than 41% of the global terrestrial area, larger than that of forests [1]. Furthermore, 10%–20% of these drylands face severe degradation, which is accelerated by climate change and population growth. In countries including China and Mongolia where more than 250 million people are directly affected by desertification, the efforts to prevent this expansion and to rehabilitate degraded areas by restoring vegetation are increasing [2–5]. Restoration of vegetation improves soil reinforcement by decreasing soil erosion and eventually decreasing or mitigating desertification [6]. To avoid failure and side effects caused by planting trees in these areas, it is necessary to select appropriate species which have already survived and adapted to the drought and harsh conditions [5,7,8].

The survival of indigenous species in arid and semi-arid areas is directly attributed to their ability to adapt to surrounding environmental conditions including water availability and heat stress [9–14]. As soil and plant water potentials decrease and vapor pressure deficit increases, plants close their stomata, the main channels for the exchange of water and CO_2 during transpiration and photosynthesis, respectively. Stomatal closure reduces water loss and preserves hydraulic conductivity to prevent cavitation and hydraulic failure. At the same time, it also causes the reduction of carbon assimilation at the foliar level. In addition, stomatal closure decreases the internal CO_2 concentration (C_i) resulting from the consumption of CO_2 by photosynthesis [15,16], thereby causing low C_i/C_a (C_a: atmospheric CO_2 concentration) in the leaf and less discrimination of ^{13}C isotope and eventually increasing the water-use efficiency of the plant, which is defined as the amount of assimilated carbon per unit water loss through transpiration [17–22]. A decrease in transpiration and consequent reduction in carbon assimilation affect the metabolism and concentrations of carbohydrates, nitrogen and other nutrients required for osmotic adjustment of plant tissues [19,23].

Such changes in physiological characteristics are often the result of structural acclimation, which is a modification of morphological traits through changes in the expression of hundreds of related genes [24]. Examples of changes under water stress include plant height reduction to decrease the water transport distance from root to leaf [25–27], increased root to shoot ratio, leaf size reduction [28,29], and development of a thick cuticle layer and dense mesophyll tissues to prevent water loss through the leaf surface [30,31]. These changes result in a higher leaf mass per leaf unit area (LMA) in low precipitation habitats [28,32–35]. In addition, stomata tend to form deep below the leaf surface as sunken stomata [36–41], and decrease their area per leaf unit area by the reduction of stomatal density, size or both [42,43].

Ulmus pumila L., which is the only elm species found in southern and southeastern Mongolia [44], is naturally distributed throughout China, Mongolia, Korea and Russia and covers a wide range of environmental gradients with average annual precipitation levels less than 100 mm to over 1300 mm [44]. Thus, *U. pumila* is one of the most commonly used species in Mongolia and Inner Mongolia, China for rehabilitating arid and semi-arid areas to combat desertification [45–47]. Previous studies on *U. pumila* have focused on seedlings due to convenience and the importance of early stage survival rates during rehabilitation [46–49]. However, there are a limited number of studies addressing morphological and physiological traits of mature *U. pumila* trees that enable them to survive in arid areas. More specifically, no studies have been conducted to analyze the effects of microenvironments within arid and semi-arid areas [50,51]. Therefore, we proposed two major hypotheses with respect to two aspects: (1) Physiological and morphological characteristics of Siberian elm will be differentiated along a variation in annual precipitation; (2) Even under a similar range of annual precipitation, the above characteristics will vary according to micro-environmental conditions. Therefore, the objectives of this study were to (1) evaluate changes in morphological and physiological characteristics of *U. pumila* along aridity index (AI) gradients under arid and mesic conditions, (2) assess the water-use efficiency of *U. pumila* growing along different AI gradients and (3) compare these characteristics within the different microenvironments of arid and semi-arid areas such as steppes, sand dunes and riversides in Mongolia and China.

2. Experimental Section

2.1. Study Sites

This study was performed in five different regions of northeast Asia, with two additional experimental sites for microenvironment comparison, and encompassed a wide range of latitude, precipitation (approximately 230–1300 mm·year^{-1}) and temperature (1–10 °C mean annual temperature). The sites used include Bayan Gobi, Mongolia (BG); Khugnukhan, Mongolia (KK); Selenge Steppe, Mongolia (ST); Selenge River, Mongolia (SR); Wulanaodu, China (WL); Qingyuan, China (QY) and Jeongseon, Korea (JS) (Figure 1). The basic information regarding these seven experimental sites, including annual precipitation and temperature, is listed in Table 1. BG and KK were considered separate experimental sites within the same region, as were ST and SR. The sites had microenvironmental differences as described below; however, BG and KK, and similarly, ST and SR, were considered to have similar climate conditions due to their close distance and the lack of available weather data to further distinguish the two sites.

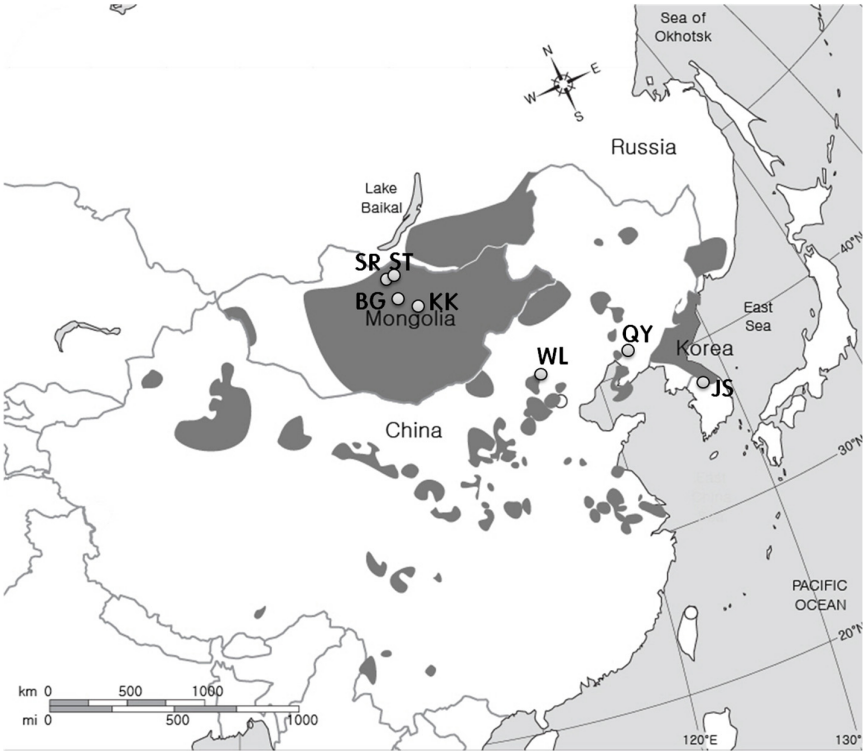

Figure 1. Natural distribution of the Siberian elm (*U. pumila* L.) and locations of seven sampling sites in Mongolia (Bayan Gobi, BG; Khugnukhan, KK; Selenge Steppe, ST; Selenge River, SR), China (Qingyuan, QY; Wulanaodu, WL) and Korea (Jeongseon, JS).

Table 1. Geographical and climatic conditions* of seven sampling sites in Mongolia (Bayang Gobi, BG; Kokunhang, KK; Selenge Steppe, ST; Selenge River, SR), China (Qingyuan, QY; Wulanaodu, WL) and Korea (Jeongseon, JS).

Country	Sampling Site	Geographical Location	Altitude (m)	Climate and Site Type	Annual Precipitation (mm)	Mean Annual Temperature (°C)	Maximum Monthly Temperature (°C)	Minimum Monthly Temperature (°C)	Aridity Index
Mongolia	Bayan Gobi (5)	47°17′16.5″ N 103°44′46.1″ E	1283	Arid climate and sand dune	232 ± 30 ** d ***	1.7 ± 0.6 d	19.7 ± 0.8c	−16.0 ± 1.0 a	19.83
	Khugnukhan (5)	47°26′01.7″ N 103°40′40.1″ E	1342	Arid climate and wood land	232 ± 30 d	1.7 ± 0.6 d	19.7 ± 0.8 c	−16.0 ± 1.0 a	19.83
	Selenge steppe (4)	50°09′03.6″ N 106°12′37.4″ E	630	Semi-arid climate and wood land	251 ± 17	1.2 ± 0.2	22.1 ± 0.3	−24.5 ± 0.3	22.41
	Selenge riverside (4)	50°03′54.7″ N 106°09′02.3″ E	614	Semi-arid climate and riverside	251 ± 17	1.2 ± 0.2	22.1 ± 0.3	−24.5 ± 0.3	22.41
China	Wulanaodu (3)	43°04′53.8″ N 119°36′33.2″ E	537	Semi-arid climate and sand dune	329 ± 35 c	6.6 ± 0.6 b	25.9 ± 3.2 b	−14.4 ± 1.3 ab	19.82
	Qingyuan (2)	41°54′57.2″ N 124°55′13.1″ E	607	Warm temperate climate and valley in forest	730 ± 123 b	5.1 ± 0.5 c	23.9 ± 5.7 a	−11 ± 1.7 b	48.34
Korea	Jeongseon (1)	37°16′16.6″ N 128°35′31.0″ E	242	Warm temperate climate and valley in forest	1304 ± 103 a	10.1 ± 0.1 a	23.2 ± 0.8 a	−4.3 ± 0.7 c	64.88

* Climate data from 2007–2010 were cited from (1) The Annual Report of Automatic Weather Station Data (527 Jeongseon) Korea Meteorological Administration, Korea; (2) Qingyuan Experimental Station of Forest Ecology of Institute of Applied Ecology, Chinese Academy of Sciences, and Yang et al. [52]; (3) Wulanaodu Desertification Experiment Station of Chinese Academy of Sciences, Yan et al. [53], and Ma et al. [54]; (4) Institute of Meteorology, Mongolian Academy of Sciences; (5) Gurvanbulag sum, Weather station data. ** SE: Standard error. *** Different letters denote significant differences according to Duncan's multiple range tests at the 5% level of probability.

BG and KK were located in the midwestern part of Mongolia, approximately 17 km apart, encompassing sand dunes and woodlands, respectively. At both sites, the Siberian elm was the only tree species, and the understory was composed of shrubs such as *Caragana microphylla* Lam., *Ephedra siinica* Stapf., *Polygonum sericeum* Pall. ex Georgi and *Leymus racemosus* Lam. The closest weather station was within 20 km of the experimental sites, and it reported the lowest precipitation totals (232 ± 30 mm·year^{-1}) during the years 2007–2010.

The other similar sites, ST and SR, were located on a steppe (ST) and a riverside (SR), respectively, in Selenge in northern Mongolia. The sites were located 8 km apart, and their average annual precipitation and temperature values during 2000–2009 were collected by the Institute of Meteorology, Mongolian Academy of Sciences.

Site WL in northeastern Inner Mongolia exhibited a semi-arid climate with an annual precipitation of approximately 300 mm·year^{-1} (Wulanaodu Desertification Experiment Station of Chinese Academy of Sciences, 2007–2010; Table 1). Siberian elms were the only trees in the area and were scattered over sand dunes and grasslands.

Site QY, which had the second highest precipitation (730 ± 123 mm·year^{-1}), was located on the hillside of a steep mountainous region in eastern Liaoning Province, China (Qingyuan Experimental Station of Forest Ecology of Chinese Academy of Sciences, 2007–2010, Table 1) that had a stream flowing in the valley below. However, this site was located sufficiently high enough so that it never flooded during severe rain events. The climate of this region was typical of a continental monsoon region with humid, rainy summers and cold, dry winters [52].

Site JS was located in the Dong River valley, a temperate deciduous forest zone, and had the highest annual precipitation (1304 ± 103 mm·year^{-1}). More than 50% of the total annual precipitation occurred during the summer months (June to August) (Korea Meteorological Administration, 2007–2010) and frequently occurred in the form of severe thunderstorms and typhoons. As a result, trees that grew along the riverbank within the steep, sloped and narrow valley experienced occasional floods above tree height during localized torrential downpours [55].

Based on their microenvironment, BG and WL were categorized as sand dunes, and ST and KK were considered steppes. SR was the only site categorized as a riverside. Although JS was also located on the side of a river, it was categorized as a forest area because it was similar to the mesic forest at site QY.

2.2. Aridity Index

To account for environmental variables other than P, such as air temperature, aridity indexes (AI) were calculated with monthly to yearly modification from Zhang et al. [38] as below:

$$\mathrm{AI} = \frac{P}{\mathrm{MAT} - 10} \quad (1)$$

AI is the aridity index and MAT indicates mean annual temperature (°C). In accordance with the above equation, a lower AI value signifies a more arid condition.

2.3. Sample Collection

During the late growing season (late August to early September), a minimum of 15 trees over 60 years of age were selected at each site based on the number of tree rings (data not shown) and both height and diameter at breast height (DBH) measurements. Twenty sun leaves, located at mid-height of the crown outer envelope and fully exposed to sunlight, were obtained from a minimum of 12 trees per site. A total of at least 200 leaves were collected from each site. The sampled leaves were sealed in plastic bags with silica gel and stacked between flat newspaper to prevent any potential damage by insects and decay. The samples were stored at room temperature until analysis.

2.4. Leaf Mass per Leaf Unit Area (LMA)

The LMA was calculated by dividing the dry leaf mass by the leaf area for all sampled leaves from each site [27]. To obtain the dry leaf mass, the leaves were dried in a drying oven at 72 °C for at least 48 h and then weighed to within 0.01 g using an electronic microscale (Precision Balance AR2130, Ohaus Corp., Parsippany, NJ, USA). The area of an individual leaf was measured using an LI-3100C Portable Leaf Area Meter prior to drying in the oven (LI-COR, Lincoln, NE, USA).

2.5. Leaf Thickness and Stomatal Size, Density and Area per Unit Leaf Area

Leaf thickness and stomata were observed with a Photomicroscope (ZEISS Axiophot, Germany). Five fragments of a leaf's midsection were fixed in resin blocks and sectioned for microscopy. Leaf thickness was measured five times for each fragment, and the average value was calculated. Leaf surface impressions for investigating stomatal morphology were made using the nail polish method [56]. The lower side of the leaf samples were painted with clear nail polish and allowed to dry thoroughly. Once dry, a square strip of dried nail polish was gently peeled from the leaf and attached to a piece of clear plastic packaging tape. The leaf impressions were taped to a clean glass slide for observation using the Photomicroscope. Stomata were counted within 30 separate areas (each 451.92 μm × 338.65 μm), and the stomatal density per square millimeter was calculated. The stomatal size was determined by multiplying the length (μm) and width (μm) of the stomata. The stomatal area per leaf unit area (A_S/A_L) was calculated by multiplying the stomatal size and stomata density [42].

2.6. Intrinsic WUE

Six leaves (one leaf per tree) were collected from each site and dried in an oven at 72 °C for at least 48 h. The dried samples were homogenized by grinding them to a powder using FastPrep-24 (MP Biomedicals, Santa Ana, CA, USA). Analysis of $\delta^{13}C$ was performed at the National Instrumentation Center for Environmental Management (NICEM), College of Agriculture and Life Sciences (CALS), Seoul National University, Republic of Korea.

The C_i/C_a ratio was calculated using the equation in Farquhar et al. [57] with some modification by Korol et al. [58] as shown below:

$$C_i/C_a = \frac{(\delta_{atm} - \delta^{13}C - a)}{(b - a)} \quad (2)$$

In the equation, δ_{atm} indicates the $^{13}CO_2$ discrimination in the air (−7.8‰), a represents the diffusivity of $^{13}CO_2$ in air (mol) (4.4‰), and b represents the amount of discrimination of C_3 leaves against $^{13}CO_2$ with respect to the ribulose bisphosphate carboxylase/oxygenase (27‰).

The intrinsic WUE was calculated using the equation in Saurer et al. [59] as shown below:

$$WUE(\mu mol\ mol^{-1}) = \frac{(C_a - C_i)}{1.6} \quad (3)$$

Here, C_a indicates the ambient CO_2 concentration (390 ppm) and C_i indicates the intercellular CO_2 concentration (ppm), which is estimated from Equation (2).

2.7. Statistical Analysis

Statistical analysis was performed using SPSS software (version 16.0, SPSS Inc., Chicago, IL, USA). Differences in the mean values of morphological and physiological variables were analyzed using ANOVA after the Shapiro-Wilk normality test, and multiple comparisons were performed using Duncan's multiple range tests [60]. An estimation of the derived parameters, such as leaf size, LMA, A_S/A_L and WUE, was performed and plotted using Sigma Plot 2011 (version 12.0, SPSS Inc., USA).

3. Results and Discussion

3.1. Environment and Aridity Index

Several environmental variables, in addition to *P* gradients, differed significantly between sites (Table 1). In general, mean annual temperature and minimum monthly temperature increased as the latitude of the experimental site decreased. However, WL, located in an arid sand dune, had higher mean and maximum monthly temperatures than QY, a temperate forest site located at lower latitude (6.6 ± 0.6 vs. 5.1 ± 0.5 and 25.9 ± 3.2 vs. 23.9 ± 5.7 °C, respectively). WL also had greater temperature fluctuations and a lower minimum monthly temperature than QY. These temperature differences justified the use of AI in WL classifications as opposed to *P* alone, especially in arid and semi-arid sites. WL had a more arid environment than ST and SR, even though ST and SR had approximately 80 mm·year^{-1} less precipitation than WL. Therefore, *P* was still the most decisive factor, and AI showed a strong positive relationship with *P* (AI = 0.044 *P* + 10.26, *p*-value < 0.0001, Figure 2). However, the relationship was not strong in the arid region. In our study, five out of seven sites (BG, KK, SR, ST and WL) had an AI below 25 and were thus considered arid regions [61]. The other two sites, QY and JS, had AI values of 48.3 and 64.9, respectively, and were categorized as mesic (Table 1).

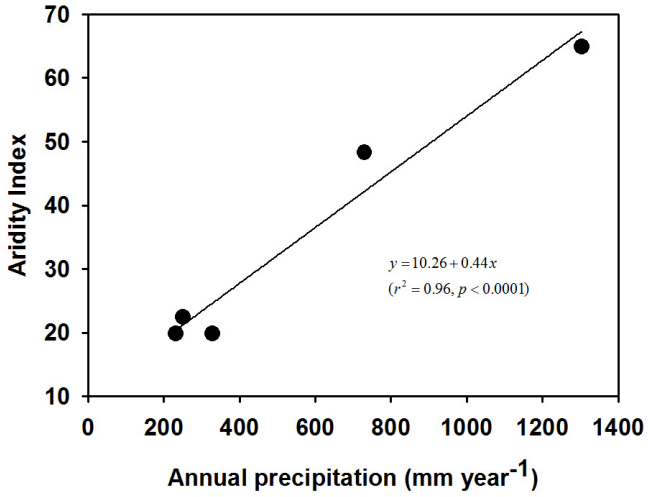

Figure 2. Correlation between annual precipitation and aridity index.

3.2. Height and DBH

The heights and DBH of the trees differed significantly among the sites, especially between temperate (QY and JS) and arid sites (BG, KK, SR, ST and WL) (Figure 3A, B). The average tree height was highest in QY (16.23 ± 1.09 m), which was the second moistest site. The second highest tree heights were recorded in the moistest site, JS (11.89 ± 0.42 m) and were followed by KK (8.01 ± 0.44) and the other arid sites, where AI and *P* were less than 25 and 400 mm·year^{-1}, respectively. However, there was no significant difference among the microenvironments of the arid sites (*p*-value = 0.24).

In contrast to height, the average DBH did not show any correlation to AI, even though the three most arid sites (KK, BG and WL) had the three largest DBH values (Figure 3B). In addition, the exact ages of the trees, other than knowing that the trees were over 60 years old, could not be obtained due to the hollow heartwood in some trees. Therefore, the ratio between height and DBH was used for further analysis instead of DBH alone. Figure 3C shows the ratio between height and DBH with a correlation between tree height and DBH. The heights of trees in the temperate forest were more than 40 times greater than DBH (80 times in QY and 45 times in JS), but trees in arid areas had values between 25 and 30 without significant differences among sites (*p*-value = 0.20202). There was no difference among arid sites (Table 2).

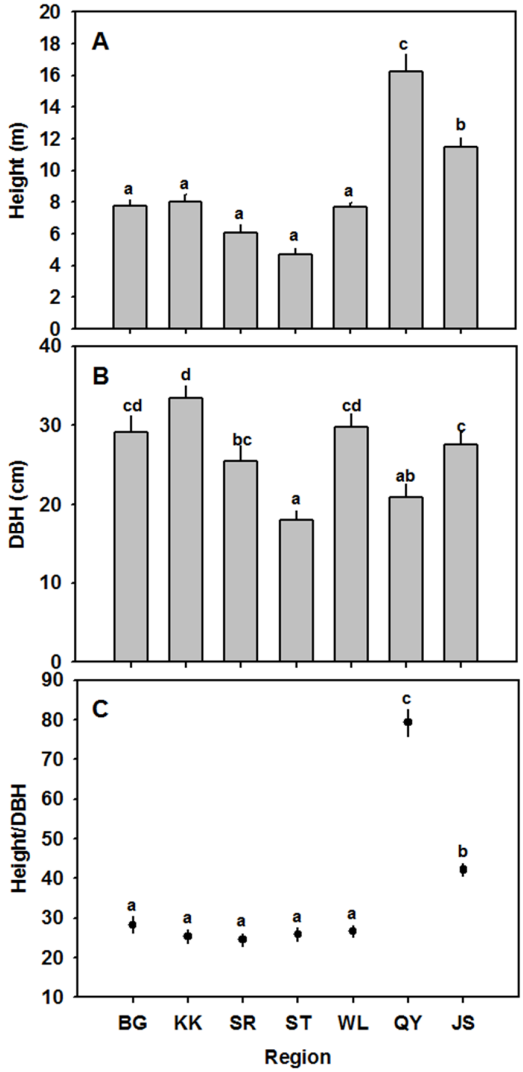

Figure 3. Comparison of the growth characteristics of Siberian elm from Mongolia (Bayan Gobi, BG; Khugnukhan, KK; Selenge Steppe, ST; Selenge River, SR), China (Qingyuan, QY; Wulanaodu, WL) and Korea (Jeongseon, JS). (**A**) The average heights; (**B**) The average diameter; (**C**) The average ratio of height to diameter. The different letters indicate significant differences according to Duncan's multiple range tests at a 5% significance level.

Shorter tree height during water shortages (Figure 3A,C) would be beneficial for the survival of Siberian elm under dry conditions, not only by decreasing the risk of wind fall, especially in the high windy areas of the Mongolian desert, but also by changing the hydraulic characteristics of trees. The shorter trees in drier regions could have a lower soil-leaf potential gradient (ψ_S–ψ_L) due to a lower gravitational water potential and increased leaf-specific hydraulic conductance [27,62–67]. Such adjustments in hydraulics enabled trees in arid areas to have a higher sap flux density and stomatal conductance than the same species in mesic areas, particularly when the vapor pressure deficit was low [27,65]. Thus, trees in arid areas would be able to sequester substantial amounts of carbon while environmental conditions were favorable, such as during the morning hours prior to stomatal closure [12,13,68–72].

Table 2. ANOVA for the growth, leaf traits and WUE characteristics of the Siberian elm in the seven study sites and three types of microenvironments.

Sampling Site	Climate Type	H	DBH	H/DBH	LMA	LS	LT	CT	PT	SS	SD	A_S/A_L	WUE
		(m)	(cm)		($g \cdot cm^{-2}$)	(cm^2)	(μm)	(μm)	(μm)	(μm^2)	(numbers mm^{-2})	($mm \cdot mm^{-1}$)	($\mu mol \cdot mol^{-1}$)
BG	Arid	7.73 ± 0.42 a	29.16 ± 1.99 cd	28.27 ± 2.09 a	0.015 ± 0.00051 cd	5.87 ± 0.34 a	342.76 ± 5.53	9.29 ± 0.30 ab	234.67 ± 6.85	930.30 ± 54.16 b	221.77 ± 11.16 a	0.20 ± 0.0089 a	71.57 ± 7.00 b
KK	Arid	8.01 ± 0.44 a	33.38 ± 1.61 d	25.33 ± 1.72 a	0.013 ± 0.00034 bc	8.42 ± 0.63 ab	294.11 ± 9.44	8.78 ± 9.44 ab	179.47 ± 8.21	895.62 ± 28.52 b	208.48 ± 16.24 a	0.19 ± 0.013 a	90.48 ± 5.49 c
ST	Semi-arid	6.07 ± 0.50 a	25.46 ± 1.94 bc	24.52 ± 1.60 a	0.014 ± 0.00075 cd	11.74 ± 0.90 bc	325.73 ± 73.02	7.63 ± 0.37 a	171.96 ± 31.27	1034.94 ± 51.33 c	185.15 ± 4.91 a	0.19 ± 0.0094 a	69.08 ± 4.96 b
SR	Semi-arid	4.67 ± 0.45 a	17.99 ± 1.26 a	25.90 ± 1.72 a	0.012 ± 0.00092 ab	9.04 ± 0.57 c	306.69 ± 22.02	10.26 ± 1.40 b	207.44 ± 18.38	861.80 ± 48.03 b	176.47 ± 6.37 a	0.15 ± 0.0096 a	67.16 ± 1.35 b
WL	Semi-arid	7.67 ± 0.90 a	29.79 ± 1.62 cd	26.65 ± 1.40 a	0.015 ± 0.00059 d	7.67 ± 0.43 ab	-	-	-	749.97 ± 3.87 a	399.78 ± 30.90 b	0.30 ± 0.022 b	87.50 ± 3.90 c
QY	Mesic	16.23 ± 1.09 c	20.91 ± 1.69 ab	79.24 ± 3.42 c	0.012 ± 0.00058 ab	12.00 ± 2.18 c	-	-	-	1043.28 ± 19.34c	431.92 ± 25.63 b	0.45 ± 0.033 c	61.91 ± 3.73 b
JS	Mesic	11.89 ± 0.42 b	27.55 ± 1.54 c	42.15 ± 1.45 b	0.011 ± 0.00039 a	11.67 ± 0.90 c	292.45 ± 9.05	7.03 ± 0.38a	187.48 ± 24.32	701.79 ± 11.78 a	642.87 ± 26.11 c	0.45 ± 0.022 c	32.90 ± 3.06 a
p-value		<0.0001	<0.0001	<0.0001	<0.0001	<0.0001	0.194	0.046	0.14	<0.0001	<0.0001	<0.0001	<0.0001
Microenvironment		**H**	**DBH**	**H/DBH**	**LMA**	**LS**	**LT**	**CT**	**PT**	**SS**	**SD**	**A_S/A_L**	**WUE**
		(m)	(cm)		($g \cdot cm^{-2}$)	(cm^2)	(μm)	(μm)	(μm)	(μm^2)	(numbers mm^{-2})	($mm \cdot mm^{-1}$)	($\mu mol \cdot mol^{-1}$)
Sand dune		7.70 ± 0.25 b	29.48 ± 1.27	27.46 ± 1.25	0.015 ± 0.00039 c	6.75 ± 0.31 a	342.76 ± 5.53	9.29 ± 0.30	234.67 ± 6.85 b	835.63 ± 34.20 a	310.78 ± 25.93 b	0.22 ± 0.017 b	79.48 ± 4.51
Steppe area		6.61 ± 0.40 ab	26.97 ± 0.40	25.57 ± 1.22	0.013 ± 0.00031 a	8.53 ± 0.52 b	311.67 ± 18.49	8.14 ± 0.41	175.29 ± 16.87 a	965.28 ± 32.74 b	196.82 ± 8.68 a	0.19 ± 0.0080 b	78.82 ± 4.43
River side		6.07 ± 0.50 a	25.46 ± 0.50	24.52 ± 1.60	0.012 ± 0.00012 a	11.74 ± 0.90 c	306.69 ± 9.56	10.26 ± 3.13	207.44 ± 18.38 ab	861.80 ± 48.03 ab	176.47 ± 6.37 a	0.15 ± 0.0096 a	69.08 ± 4.96
p-value		0.018	0.25	0.35	<0.0001	<0.0001	0.328	0.138	0.061	0.025	<0.0001	0.003	0.35

H: height, DBH: diameter at breast height, H/DBH: height to DBH ratio, LMA: leaf mass per leaf unit area, LS: leaf size, LT: leaf thickness, CT: cuticle layer thickness, PT: palisade layer thickness, SS: stomatal size, SD: stomatal density, A_S/A_L: stomatal area per leaf unit area, WUE: water use efficiency; SE: Standard error; Different letters denote significant differences according to Duncan's multiple range tests at the 5% level of probability; The minimum number of samples from each site for H, DBH and H/DBH: 12, LMA and LS: 20, LT, CT, and PT: 5, SS, SD and A_S/A_L: 10, WUE: 6.

3.3. Variation in Leaf Size, LMA and Leaf Thickness

The average leaf size increased logarithmically with the aridity index (Leaf size = 3.98 × ln(AI) − 4.22, p-value = 0.0168, Figure 4A), and there were significant differences among tree leaves in arid sites with different microenvironments (Table 2). Trees in the mesic forests of JS and QY had larger leaves (11.67 ± 0.90 cm^2 and 12.00 ± 2.18 cm^2, respectively) than trees in all arid areas except SR, which was located on a riverside. Leaves in SR were significantly larger than in other arid sites, including sand dunes and steppes (Table 2).

A reduction in leaf size can provide an efficient way for the Siberian elm to cope with hot and dry weather conditions by reducing heat stress through convective cooling of the leaf surface temperature [73,74]. Small leaves have higher boundary layer conductance than large leaves. This high boundary layer conductance increases the leaves' coupling with their surroundings, and as a result, prevents the leaf surface temperature from reaching more than 2 °C above the atmospheric temperature [74–76]. Considering that the hydraulic resistance of a leaf constitutes on average between 30% and 90% of the total plant hydraulic resistance, small leaf size and consequently a shorter traveling distance within minor and fine veins increases the hydraulic and stomatal conductance [77,78]. In addition, a decrease in leaf size helps minimize photosynthesis loss during drought. As shown by Brèda et al. [79], trees under water and heat stress compensated for photosynthesis by having a smaller leaf size with the same leaf area index as leaves formed during mesic years.

The value of LMA declined as the aridity index increased (LMA = 0.016 + (-8.0630×10^{-5}) × AI, r^2 = 0.65, p-value = 0.0282, Figure 4B) and there were significant differences in LMA values among arid sites with different microenvironments (Table 2). The highest value of LMA (153.9 $g \cdot cm^{-2}$) was obtained from WL, a sand dune site, which had leaves with statistically higher LMA values than leaves from the steppes and riverside (Table 2). The lowest LMA value (108.3 $g \cdot cm^{-2}$), which was approximately 70% of the highest value, was obtained in JS, where the annual precipitation was the highest among the study sites (1304 $mm \cdot year^{-1}$, Figure 4B).

Leaf thickness at five of the sites (not including WL, an arid sand dune, and QY, a temperate forest) was not significantly different (Table 2, p-value = 0.194), even between mesic and arid areas (Table 2, p-value = 0.194). However, the cuticle layer was significantly thinner in leaves in the temperate forest than in leaves at other arid sites (Table 2, p-value = 0.046). The thickness of the palisade mesophyll layer, however, was only marginally thicker in the leaves of trees in the sand dunes and BG compared with the other microenvironments (Table 2, p-value = 0.061). An increase in LMA values, which correlates with a dense distribution of the palisade cells and thick cuticle layer, is not considered a hydraulic adjustment to dry conditions [77]. LMA is, however, one of several traits related to effective photosynthetic performance that influences net gas exchange. A flux in net gas exchange results from internal CO_2 conductance to the site of carboxylation, internal shading, competition among carboxylation sites and nitrogen concentration and partitioning [28,33–35,76,80–82]. Thus, a large proportion of high LMA species are from desert areas, open shrub lands or woodlands where drought, nutrient limitations or both strongly inhibit tree growth [28,83].

Increased LMA and a thick cuticle layer in leaves at the arid sites, in addition to microenvironmental conditions, especially differences in leaf LMA and cuticle layer between sand dune, steppes and riverside (Table 2 and Figure 4B), could help *U. pumila* survive periods of environmental stress by providing protective mechanisms. Several studies have shown an increase in total structural carbon and lignin with high LMA, while others have shown a decrease in organic acids, minerals and proteins [84,85]. Increased structural carbon and lignified tissue are important for leaf toughness, tolerance to low water potential and resistance to herbivores [86–89].

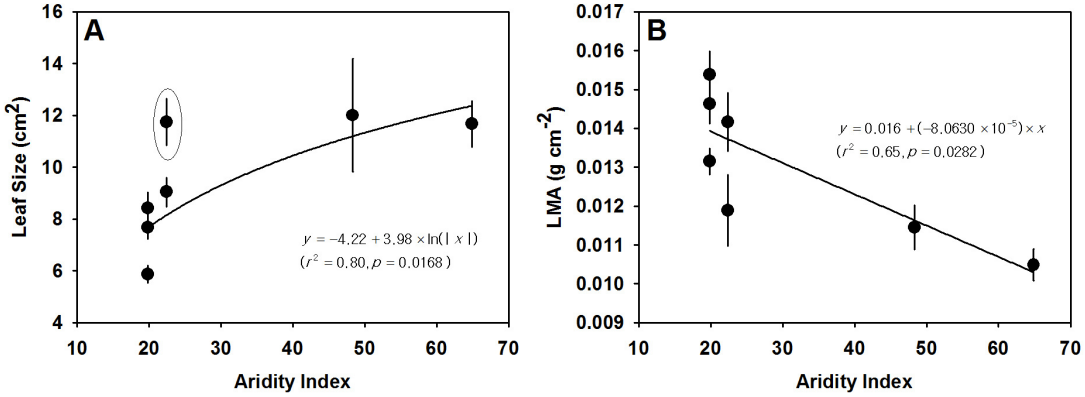

Figure 4. Comparison of the leaf characteristics from seven sampling sites. (**A**) Individual leaf size (cm^2). The line indicates logarithmic regression of leaf size (cm^2) based on the aridity index. The error bar is one standard error. The statistics were calculated excluding the circled site; (**B**) Leaf mass per unit leaf area ($g \cdot m^{-2}$, LMA). The line indicates the linear regression of the LMA ($g \cdot m^{-2}$) based on average annual precipitation.

3.4. Variation in A_S/A_L

The stomata were present only on the abaxial (lower) leaf surface at all study sites. They were all oval-shaped (Figure 5A), but significant differences were found in stomatal width, length and size in leaves from the various study sites (p-value < 0.0001, Figure 5B). Although there was no apparent relationship between stomatal size and aridity, stomatal density showed a significant correlation with aridity ($D_S = -675.65 + 301.15 \times \ln(|AI|)$, $r^2 = 0.72$, p-value = 0.0158, Figure 5C). Trees at the site with the most precipitation, JS, had three times more stomata than those at the riverside site in SR. Trees at sand dune sites (WL & KK) had higher stomatal density than that within other microenvironments (maximum p-value = 0.009).

The stomatal area per unit leaf area (A_S/A_L) also increased as the aridity index increased (as the annual precipitation increased with a plateau over 700 mm) ($A_S/A_L = -0.5 + 0.23 \times \ln(AI)$, $r^2 = 0.81$, p-value = 0.0061, Figure 5D). Similar to stomatal density, tree leaves in sand dune areas had higher A_S/A_L than those in other arid microenvironments (maximum p-value = 0.035), while those at the riverside site, SR, had the lowest value.

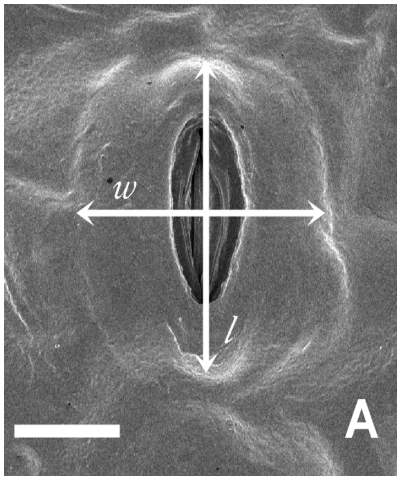

Figure 5. *Cont.*

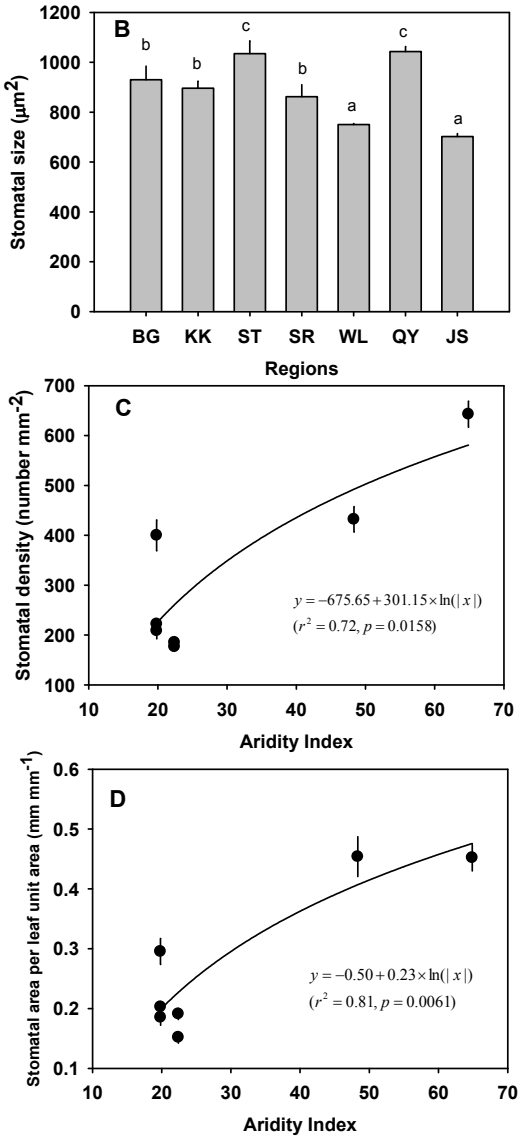

Figure 5. (**A**) Image of Siberian elm stomata from JS. *w* is stomata width, and *l* is stomata length. Bar = 10 μm; (**B**) Average size (width × length); (**C**) The stomatal density along the aridity index gradients from the seven previous sites; (**D**) The stomatal area per unit leaf area along the aridity index gradients from the seven previous sites.

Stomatal size, density and area per unit leaf area are important factors in controlling the rate of photosynthesis through stomatal conductance, and they are especially important for determining the maximum stomatal conductance. A number of studies reported that smaller stomata, with their higher cell surface area to volume ratio, responded faster to environmental changes, and in combination with high stomata density, were more efficient in reaching maximum or normal operating conductance under favorable conditions and in closing rapidly under harsh environments [29,37,43,90,91]. Although *U. pumila* showed no significant relationship between stomatal size and aridity index, the stomatal density and stomatal area increased significantly as the aridity index increased (Figure 5B–D). However, the leaves of trees on sand dunes had an overall smaller stomatal size than those in steppes and by riversides (although not significantly different) and a significantly larger stomatal density and area (Table 2). The combination of smaller stomatal size and larger stomatal density could potentially help *U. pumila* in sand dune areas respond faster to environmental changes, especially with their additional small leaf size (Table 2).

3.5. Variation of Intrinsic WUE

The intrinsic WUE of the Siberian elm, calculated using the equation in Saurer et al. [59], was different at each site (p-value < 0.0001, Table 2) and decreased as AI increased (WUE = 97.11 + (−0.92) × *AI*, r^2 = 0.76, p-value = 0.0102, Figure 6). The WUE of Siberian elm from the riverside, steppes and sand dunes was higher, with average values of 69.08 ± 4.96, 78.82 ± 4.43 and 79.48 ± 4.51 (μmol CO_2 mol^{-1} H_2O), respectively. There was no difference among arid microenvironments (p-value = 0.349).

Many studies have shown that dry-tolerant species exhibit a lower C_i/C_a value due to a less pronounced discrimination against heavier carbon, ^{13}C, than mesic species [69,92]. Generalist species, including willow and elm, have a lower minimum stomatal conductance and greater WUE than wetland species [93]. In our study, intrinsic WUE was negatively correlated with the mean annual precipitation and aridity index, indicating that the Siberian elm responded to dry conditions by using intracellular CO_2 and closing their stomata (Figure 6). However, we could not find any significant differences in WUE among arid sites, most likely because the carbon isotope composition is determined not only by water availability but also stomatal limitation. Interestingly, although stomatal density and area were higher in tree leaves in the sand dunes than in the steppes and riverside, the WUE in these different arid microenvironments did not differ (Table 2).

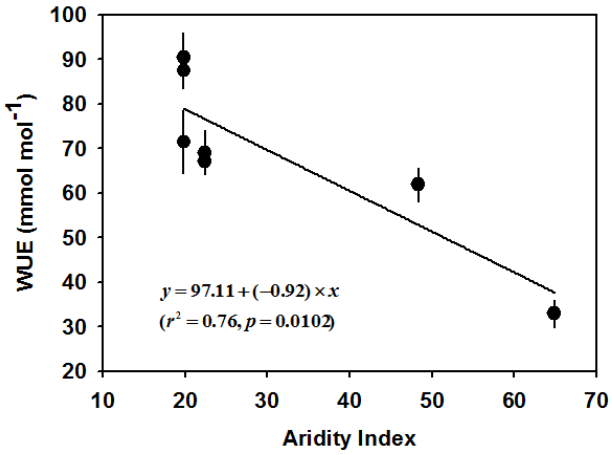

Figure 6. Water-use efficiency (WUE) of the Siberian elm leaf samples. The line indicates regressions of WUE versus annual precipitation (r^2 = 0.76).

We also compared our foliar $\delta^{13}C$ data to those of Stewart et al. [18], who found a strong relationship between the $\delta^{13}C$ values averaged for each of their study sites where annual precipitation ranged from 350 to 1700 mm. A total of 348 species from 12 families was used (Figure 7). Although our study sites showed a stronger discrepancy than the average data set of Stewart et al. [18], they were generally within the same range as sites with similar precipitation levels. *U. pumila* also showed a linear decrease in $\delta^{13}C$ with increasing precipitation from 300 to 1300 mm·$year^{-1}$. However, Schulze et al. [19] reported that the 'community-averaged' carbon isotope value remained constant between 450 and 1800 mm of rainfall. In our studies, among arid and semi-arid areas where annual precipitation is less than 400 mm·$year^{-1}$, the $\delta^{13}C$ of *U. pumila* was lower than that reported by Schulze et al. [19]. Thus, *U. pumila* showed more efficient water usage than the average community studied by Schulze et al. [19] and is likely the reason why these trees can survive within such a wide precipitation range.

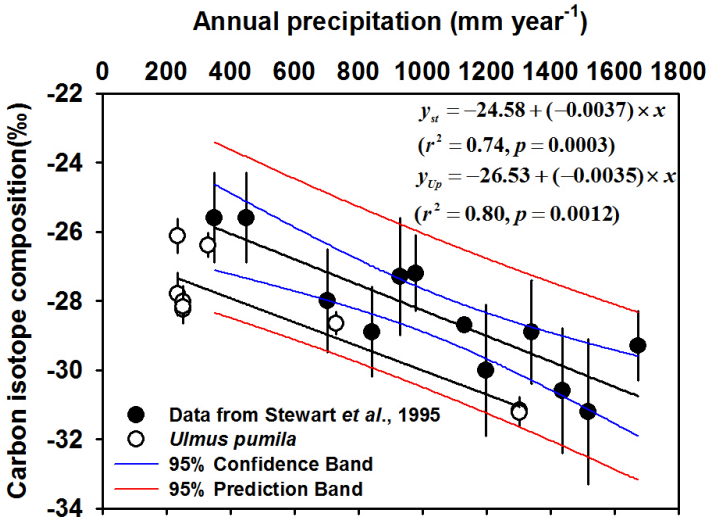

Figure 7. Carbon isotope composition (‰, $\delta^{13}C$), adopted from Stewart et al. [18], and Siberian elm leaf samples. y_{St} denotes regression data from Stewart et al. [18] and y_{Up} denotes regression of $\delta^{13}C$ in Siberian elm versus annual precipitation (mm).

4. Conclusions

The morphological and physiological differences of the mature Siberian elm trees across mesic and arid habitats, encompassing a variety of microenvironments, are highlighted in this study. Mature Siberian elm trees display significant variation in phenotypic traits such as leaf size, LMA, A_S/A_L and intrinsic WUE along different annual precipitation gradients and aridity levels. As aridity levels decrease, Siberian elm trees appear to increase their WUE by increasing their LMA and decreasing their leaf size and A_S/A_L. In addition, among arid sites, trees on sand dunes had a smaller leaf size, higher leaf mass and thicker leaf cuticle layer than those in steppes and by a riverside. However, both stomatal density and area were higher in the leaves of trees growing on sand dunes than at any other sites. When taken together, the above results suggest that Siberian elm trees employ a variety of strategies to survive under arid conditions.

From our studies, it could be concluded that the Siberian elm can adapt to survive in a harsh water-deficient environment and is thus suitable for the rehabilitation of degraded arid areas such as those found in Mongolia, China's Inner Mongolia and North Korea. Especially considering that the Siberian elm is an indigenous species of those areas, it is recommended for use over other imported species for rehabilitation.

Acknowledgments: This study was conducted with support from the National Research Foundation of Korea's "Key Joint Research Program" and Korea Forest Service (S111212L120110). We appreciate Tsedensodnom Enkhchimeg, Zhang Min, Gaofeng, Joowon and Hanuel for accompanying us on our field surveys and Seokyeol, Hyunjoo and Dawoon for helping us with laboratory experiments.

Author Contributions: Go Eun Park and Don Koo Lee conceived the study. Go Eun Park designed the study and carried out field work, data analysis and prepared the manuscript. Ki Woo Kim contributed to observe leaf structure with a microscope. Nyam-Osor Batkhuu and Jamsran Tsogtbaatar contributed to select field surveying sites and tree samples and analyzing climate data for Mongolia. Jiao-jun Zhu and Yonghuan Jin also contributed to select field sites in China and Jiao-jun Zhu contributed to analyzing climate data. Pil Sun Park and Jung Oh Hyun reviewed the work. Hyun Seok Kim performed additional data analysis and reviewed and edited the work.

Conflicts of Interest: The authors declare no conflict of interest.

References

1. Adeel, Z.; Safriel, U.; Niemeijer, D.; White, R. *Millennium Ecosystem Assessment: Ecosystems and Human Well-Being: Desertification Synthesis*; World Resource Institute: Washington, DC, USA, 2005.

2. Schlesinger, W.H.; Reynolds, J.F.; Cunningham, G.L.; Hyenneke, L.F.; Jarrell, W.M.; Virginia, R.A.; Whitford, W.G. Biological feedbacks in global desrtification. *Science* **1990**, *247*, 1043–1048. [CrossRef] [PubMed]
3. Reynolds, J.F.; Smith, D.M.S.; Lambin, E.F.; Turner, B.L., II; Mortimore, M.; Batterbury, S.P.J.; Downing, T.E.; Dowlatabadi, H.; Fernández, R.J.; Herrick, J.E. Global desertification: Building a science for dryland development. *Science* **2007**, *316*, 847–851. [CrossRef] [PubMed]
4. Intergovernmental Panel on Climate Change (IPCC). *Climate Change 2007: Synthesis Report*; The Core Writing Team, Pachauri, R.K., Reisinger, A., Eds.; Intergovernmental Panel on Climate Change: Geneva, Switzerland, 2007.
5. United Nations Convention to Combat Desertification (UNCCD). *Desertification: A Visual Synthesis*; UN Convention to Combat Desertification (UNCCD) Secretariat: Bonn, Germany, 2011; p. 50.
6. Gray, D.H.; Sotir, R. *Biotechnical and Soil Bioengineering Slope Stabilization*; John Wiley & Sons: New York, NY, USA, 1996.
7. Cao, S.X. Why large-scale afforestation efforts in China have failed to solve the desertification problem. *Environ. Sci. Technol.* **2008**, *42*, 1826–1831. [CrossRef] [PubMed]
8. Tsogtbaatar, J. Forest rehabilitation in Mongolia. In *Keep Asia Green Volume II "Northeast Asia"*; Lee, D.K., Ed.; International Union of Forest Research Organizations (IUFRO): Vienna, Austria, 2007; pp. 91–116.
9. Bray, E.A. Plant responses to water deficit. *Trends Plant Sci. Rev.* **1997**, *2*, 48–54. [CrossRef]
10. Heschel, M.S.; Sultan, S.E.; Glover, S.; Sloan, D. Population differentiation and plastic responses to drought stress in the generalist annual *Polygonum persicaria*. *Int. J. Plant Sci.* **2004**, *165*, 817–824. [CrossRef]
11. Yin, C.; Wang, X.; Duana, B.; Luob, J.; Li, C. Early growth, dry matter allocation and water use efficiency of two sympatric Populus species as affected by water stress. *Environ. Exp. Bot.* **2005**, *53*, 315–322. [CrossRef]
12. Jacobsen, A.L.; Agenbag, L.; Esler, K.J.; Pratt, R.B.; Ewers, F.W.; Davis, S.D. Xylem density, biomechanics and anatomical traits correlate with water stress in 17 evergreen shrub species of the Mediterranean-type climate region of South Africa. *J. Ecol.* **2007**, *95*, 171–183. [CrossRef]
13. Jacobsen, A.L.; Pratt, R.B.; Davis, S.D.; Ewers, F.W. Cavitation resistance and seasonal hydraulics differ among three arid Californian plant communities. *Plant Cell Environ.* **2007**, *30*, 1599–1609. [CrossRef] [PubMed]
14. Valladares, F.; Gioanoli, E.; Gòmez, J.M. Ecological limits to plant phenotypic plasticity. *New Phytol.* **2007**, *176*, 749–763. [CrossRef] [PubMed]
15. Farquhar, G.D.; Sharkey, T.D. Stomatal conductance and photosynthesis. *Annu. Rev. Plant Biol.* **1982**, *33*, 317–345. [CrossRef]
16. Lambers, H.; Chapin, F.S.; Pons, T.L. *Plant Physiological Ecology*, 2nd ed.; Springer: New York, NY, USA, 2008; p. 604.
17. Aber, J.D.; Driscoll, C.T. Effects of land use, climate variation and N deposition on N cycling and C storage in northern hardwood forests. *Glob. Biogeochem. Cycles* **1997**, *11*, 639–648. [CrossRef]
18. Stewart, G.R.; Turnbull, M.H.; Schmidt, S.; Erskine, P.D. ^{13}C natural abundance in plant communities along a rainfall gradient: A biological integrator of water availability. *Aust. J. Plant Physiol.* **1995**, *22*, 51–55. [CrossRef]
19. Schulze, E.D.; Williams, R.J.; Farquhar, G.D.; Schulze, W.; Langridge, J.; Miller, J.M.; Walker, B.H. Carbon and nitrogen isotope discrimination and nitrogen nutrition of trees along a rainfall gradient in northern Australia. *Aust. J. Plant Physiol.* **1998**, *25*, 413–425. [CrossRef]
20. Chaves, M.M.; Osorio, J.; Pereira, J.S. Water use efficiency and photosynthesis. In *Water Use Efficiency in Plant Biology*; Bacon, M.A., Ed.; Blackwell Publishing: Hoboken, NJ, USA, 2004.
21. Zhao, L.; Xiao, H.; Liu, X.; Li, J.; Xiao, S. Foliar stable carbon isotope discrimination and nutrients contents in two desert plant species. *Pol. J. Ecol.* **2007**, *55*, 57–66.
22. Yanqi, S.; Fei, Y.; Xiaoyong, C.; Fulai, L. Plasticity in stomatal size and density of potato leaves under different irrigation and phosphorus regimes. *J. Plant Physiol.* **2014**, *171*, 1248–1255.
23. Tomlinson, K.W.; Poorter, L.; Sterck, F.J.; Borghetti, F.; Ward, D.; Bie, S.; Langevelde, F. Leaf adaptations of evergreen and deciduous trees of semi-arid and humid savannas on three continents. *J. Ecol.* **2013**, *101*, 430–440. [CrossRef]

24. Street, N.R.; Skogström, O.; Sjödin, A.; Tucker, J.; Rodrı´guez-Acosta, M.; Nilsson, P.; Jansson, S.; Taylor, G. The genetics and genomics of the drought response in Populus. *Plant J.* **2006**, *48*, 321–341. [CrossRef] [PubMed]
25. Ryan, M.G.; Yoder, B.J. Hydraulic limits to tree height and tree growth. *Bioscience* **1997**, *47*, 235–242. [CrossRef]
26. Mencuccini, M. The ecological significance of long-distance water transport: Short-term regulation, long-term acclimation and the hydraulic costs of stature across plant life forms. *Plant Cell Environ.* **2003**, *26*, 163–182. [CrossRef]
27. Addington, R.N.; Donovan, L.A.; Mitchell, R.J.; Vose, J.M.; Pecot, S.D.; Jack, S.B.; Hacke, U.G.; Sperry, J.S.; Oren, R. Adjustments in hydraulic architecture of *Pinus palustris* maintain similar stomatal conductance in xeric and mesic habitats. *Plant Cell Environ.* **2006**, *29*, 535–545. [CrossRef] [PubMed]
28. Poorter, H.; Niinemets, U.; Poorter, L.; Wright, I.J.; Villar, R. Causes and consequences of variation in leaf mass per area (LMA): A meta-analysis. *New Phytol.* **2009**, *182*, 565–588. [CrossRef] [PubMed]
29. Mao, P.; Zang, R.; Shao, H.; Yu, J. Functional trait trade-offs for the tropical montane rain forest species responding to light from simulating experiments. *Sci. World J.* **2014**, *2014*, 1–9. [CrossRef] [PubMed]
30. Ennajeh, M.; Vadel, A.M.; Cochard, H.; Khemira, H. Comparative impacts of water stress on the leag anatomy of a drought-resistant and a drought-sensitive olive cultivar. *J. Hortic. Sci. Biotechnol.* **2010**, *85*, 289–294. [CrossRef]
31. Zhang, J.L.; Poorter, L.; Cao, K.F. Productive leaf functional traits of Chinese savanna species. *Plant Ecol.* **2012**, *213*, 1449–1460. [CrossRef]
32. Abrams, M.D.; Kubiske, M.E.; Mostoller, S.A. Relating wet and dry year ecophysiology to leaf structure in contrasting temperate tree species. *Ecology* **1994**, *75*, 123–133. [CrossRef]
33. Wright, I.J.; Reich, P.B.; Westoby, M. Strategy-shifts in leaf physiology, structure and nutrient content between species of high and low rainfall, and high and low nutrient habitats. *Funct. Ecol.* **2001**, *15*, 423–434. [CrossRef]
34. Santiago, L.S.; Kitajima, K.; Wright, S.J.; Mulkey, S.S. Coordinated changes in photosynthesis, water relations and leaf nutrional traits of canopy trees along a precipitation gradient in lowland tropical forest. *Oecologia* **2004**, *4*, 495–502. [CrossRef] [PubMed]
35. Schulze, E.D.; Turner, N.C.; Nicolle, D.; Schumacher, J. Species differences in carbon isotope ratios, specific leaf area and nitrogen concentrations in leaves of Eucalyptus growing in a common garden compared with along an aridity gradient. *Physiol. Plant.* **2006**, *127*, 434–444. [CrossRef]
36. Willmer, C.; Fricker, M. *Stomata*, 2nd ed.; Chapman and Hall: London, UK, 1996; p. 375.
37. Franks, P.J.; Drake, P.L.; Beerling, D.J. Plasticity in maximum stomatal conductance constrained by negative correlation between stomatal size and density: An analysis using *Eucalyptus globulus*. *Plant Cell Environ.* **2009**, *32*, 1737–1748. [CrossRef] [PubMed]
38. Zhang, Q.; Xu, C.-Y.; Zhang, Z. Observed changes of drought/wetness episodes in the Pearl River basin, China, using the standardized precipitation index and aridity index. *Theor. Appl. Climatol.* **2009**, *98*, 89–99. [CrossRef]
39. Franca, M.G.C.; Prados, L.M.Z.; Lemos-Filho, J.P.; Ranieri, B.D.; Vale, F.H.A. Morphological differences in leaves of *Lavoisiera campos-portoana* (Melastomataceae) enhance higher drought tolerance in water shortage events. *J. Plant Res.* **2012**, *125*, 85–92. [CrossRef] [PubMed]
40. Zhang, Y.; Equiza, M.A.; Zheng, Q.; Tyree, M.T. Factors controlling plasticity of leaf morphology in *Robinia pseucoacacia* L. II: The impact of water stress on leaf morphology of seedlings grown in a controlled environment chamber. *Ann. For. Sci.* **2012**, *69*, 39–47. [CrossRef]
41. Park, G.E.; Kim, K.W.; Lee, D.K.; Hyun, J.O. Adaptive phenotypic plasticity of Siberian elm in response to drought stress: Increased stomatal pore depth. *Microsc. Microanal.* **2013**, *19* (Suppl. S5), 178–181. [CrossRef] [PubMed]
42. Herrera, A.; Cuberos, M. Stomatal size, density and conductance in leaves of some xerophytes from a thorn scrub in Venezuela differing in carbon fixation pathway. *Ecotropicos* **1990**, *3*, 67–76.
43. Venora, G.; Calcagno, F. Study of stomatal parameters for selection of drought resistant varieties in *Triticum durum* DESF. *Euphytica* **1991**, *57*, 275–283. [CrossRef]
44. Wesche, K.; Walther, D.; von Wehrden, D.; Hesen, I. Trees in the desert: Reproduction and genetic structure of fragmented *Ulmus pumila* forests in Mongolian drylands. *Flora* **2011**, *206*, 91–99. [CrossRef]
45. Dulamsuren, C.; Kamelin, R.V.; Cvelev, N.N.; Hauck, M.; Mühlenberg, M. Additions to the flora of the Khentej, Mongolia, Part 2. *Willdenowia* **2004**, *34*, 505–510. [CrossRef]

46. Shi, L.; Zhang, Z.J.; Zhang, C.Y.; Zhang, J.Z. Effects of sand burial on survival, growth, gas exchange and biomass allocation of *Ulmus pumila* seedlings in the Hunshandak Sandland, China. *Ann. Bot.* **2004**, *94*, 553–560. [CrossRef] [PubMed]
47. Dulamsuren, C.; Hauck, M.; Nyambayar, S.; Osokhjargai, D.; Leuschner, C. Establishment of *Ulmus pumila* seedlings on steppe slopes of the northern Mongolian mountain taiga. *Acta Oecol.* **2009**, *35*, 563–572. [CrossRef]
48. Jiang, C.; Jian, G.; Wang, X.; Li, L.; Biswas, D.K.; Li, Y. Increased photosynthetic activities and thermost ability of photosystem II with leaf development of elm seedlings (*Ulmus pumila*) probed by the fast fluorescence rise OJIP. *Environ. Exp. Bot.* **2006**, *58*, 261–268. [CrossRef]
49. Song, F.; Yang, C.; Liu, X.; Li, G. Effect of salt stress on activity of superoxide dismutase (SOD) in *Ulmus pumila* L. *J. For. Res.* **2006**, *17*, 13–16. [CrossRef]
50. Li, Y.G.; Jiang, G.M.; Liu, M.Z.; Niu, S.L.; Gao, L.M.; Cao, X.C. Photosynthetic response to precipitation/rainfall in predominant tree (*Ulmus pumila*) seedlings in Hunshandak Sandland, China. *Photosynthetica* **2007**, *45*, 133–138. [CrossRef]
51. Tanaka-Oda, A.; Kenzo, T.; Koretsune, S.; Sasaki, H.; Fukuda, K. Ontogenetic changes in water-use efficiency ($\delta^{13}C$) and leaf traits differ among tree species growing in a semiarid region of the Loess Plateau, China. *For. Ecol. Manag.* **2010**, *259*, 953–957. [CrossRef]
52. Yang, W.Q.; Murthy, R.; King, P.; Topa, M.A. Diurnal changes in gas exchange and carbon partitioning in needles of fast- and slow-growing families of loblolly pine (*Pinus taeda*). *Tree Physiol.* **2002**, *22*, 489–498. [CrossRef] [PubMed]
53. Yan, Q.L.; Zhu, J.J.; Hu, Z.B.; Sun, O.J. Environmental impacts of the Shelter Forests in Horqin Sandy Land, Northeast China. *J. Environ. Qual.* **2011**, *40*, 815–824. [CrossRef] [PubMed]
54. Ma, J.; Liu, Z.; Zeng, D.; Liu, B. Aerial seed bank in Artemisia species: how it responds to sand mobility. *Trees* **2010**, *24*, 435–441. [CrossRef]
55. Choung, H.L.; Kim, C.H.; Yang, K.C.; Chun, J.I.; Roh, H.C. Structural characteristics and maintenance mechanism of *Ulmus pumila* community at the Dong River, Gangwon-do, South Korea. *J. Ecol. Field Biol.* **2003**, *26*, 255–261. [CrossRef]
56. Gitz, D.C.; Baker, J.T. Methods for creating stomatal impressions directly onto archivable slides. *Agron. J.* **2009**, *101*, 232–236. [CrossRef]
57. Farquhar, G.D.; O'Leary, M.H.; Berry, J.A. On the relationship between carbon isotope discrimination and the intercellular carbon dioxide concentration in leaves. *Aust. J. Plant Physiol.* **1982**, *9*, 121–137. [CrossRef]
58. Korol, R.L.; Kirschbaum, M.U.F.; Farquar, G.D.; Jeffreys, M. Effects of water status and soil fertility on the C-isotope signature in *Pinus radiata*. *Tree Physiol.* **1999**, *19*, 551–562. [CrossRef] [PubMed]
59. Saurer, M.; Siegwolf, R.W.; Schweinfruber, F.H. Carbon isotope discrimination indicates improving water-use effieicncy of trees in northern Eurasia over the last 100 years. *Glob. Chang. Biol.* **2004**, *10*, 2109–2120. [CrossRef]
60. Duncan, D.B. Multiple range and multiple *F* test. *Biometrics* **1955**, *11*, 1–42. [CrossRef]
61. World Meteorological Organization. *Drought and Agriculture*; WMO Note 138 Publications WMO-392; WMO: Geneva, Switzerland, 1975; p. 127.
62. Sperry, J.S.; Pockman, W.T. Limitation of transpiration by hydraulic conductance and xylem cavitation in Betula occidentalis. *Plant Cell Environ.* **1993**, *16*, 279–287. [CrossRef]
63. Saliendra, N.Z.; Sperry, J.S.; Comstock, J.P. Influence of leag water status on stomatal response to humidity, hydraulic conductance, and soil drought in *Betula occidentalis*. *Planta* **1995**, *196*, 357–366. [CrossRef]
64. Bond, B.J.; Kavanagh, K.L. Stomatal behavior of four woody species in relation to leaf-specific hydraulic conductance and threshold water potential. *Tree Physiol.* **1999**, *19*, 503–510. [CrossRef] [PubMed]
65. Schäfer, K.V.R.; Oren, R.; Tenhunen, J.D. The effect of tree height on crown level stomatal conductance. *Plant Cell Environ.* **2000**, *23*, 365–375. [CrossRef]
66. Duan, B.; Yin, C.; Li, C. Responses of conifers to drought stress. *Chin. J. Appl. Environ. Biol.* **2005**, *11*, 115–122.
67. Sterk, F.H.; Zweifel, R.; Sass-Klaassen, U.; Chowdury, Q. Persisting soil drought reduces leaf specific conductiveity in Scots pine (*Pinus sylvestris*) and pubescent oak (*Quercus pubescen*). *Tree Physiol.* **2008**, *28*, 529–536. [CrossRef]
68. Martı´nez-Vilalta, J.; Prat, E.; Oliveras, I.; Piñol, J. Xylem hydraulic properties of roots and stems of nine Mediterranean woody species. *Ecophygiology* **2002**, *133*, 19–29.

69. Katul, G.; Leuning, R.; Oren, R. Relationship between plant hydraulic and biochemical properties derived from a steady-state coupled water and carbon transport model. *Plant Cell Environ.* **2003**, *26*, 339–350. [CrossRef]
70. Hacke, U.G.; Sperry, J.S.; Wheeler, J.K.; Castro, L. Scaling of angiosperm xylem structure with safety and efficiency. *Tree Physiol.* **2006**, *26*, 689–701. [CrossRef] [PubMed]
71. Sperry, J.S.; Hacke, U.G.; Pittermann, J. Size and function in conifer tracheids and angiosperm vessels. *Am. J. Bot.* **2006**, *93*, 1490–1500. [CrossRef] [PubMed]
72. Micco, V.; Aronne, G.; Baas, P. Wood anatomy and hydraulic architecture of stems and twigs of some Mediterranean trees and shrubs along a mesic-xeric gradient. *Trees* **2008**, *22*, 643–655. [CrossRef]
73. Givnish, T.J. Comparative studies of leaf form: Assessing the relative roles of selective pressures and phylogenetic constrains. *New Phytol.* **1987**, *106*, 131–160. [CrossRef]
74. Campbell, G.S.; Norman, J.M. The light environment of plant canopies. In *An Introduction to Environmental Physics*; Springer: New York, NY, USA, 1998; pp. 247–278.
75. McDwell, N.; Pockman, W.T.; Allen, C.D.; Breshears, D.D.; Cobb, S.; Kolb, T.; Plaut, J.; Sperry, J.; West, A.; Williams, D.G.; Yepez, E.A. Mechanisms of plant survival and mortality during drought: why do some plants survive while others succumb to drought? *New Phytol.* **2008**, *178*, 719–739. [CrossRef] [PubMed]
76. Montpied, P.; Granier, A.; Dreyer, E. Seasonal time-course of gradients of photosynthetic capacity and mesophyll conductance to CO_2 across a beech (*Fagus sylvatica* L.) canopy. *J. Exp. Bot.* **2009**, *60*, 2407–2418. [CrossRef] [PubMed]
77. Sack, L.; Holbrook, N.M. Leaf hydraulics. *Annu. Rev. Plant Biol.* **2006**, *57*, 361–381. [CrossRef] [PubMed]
78. Murphy, M.R.C.; Jordan, G.J.; Brodribb, T.J. Differential leaf expansion can enable hydraulic acclimation to sun and shade. *Plant Cell Environ.* **2012**, *35*, 1407–1418. [CrossRef] [PubMed]
79. Brèda, N.; Huc, R.; Granier, A.; Dreyer, E. Temperate forest trees and stands under severe drought: A review of ecophysiological responses, adaptation processes and long-term consequences. *Ann. For. Sci.* **2006**, *63*, 625–644. [CrossRef]
80. Reich, P.B.; Ellsworth, D.S.; Walters, M.B. Leaf structure (specific leaf area) modulates photosynthesis-nitrogen relations: evidence from within and across species and functional groups. *Funct. Ecol.* **1998**, *12*, 948–958. [CrossRef]
81. Tarémolières, M.; Schnitzler, A.; Sánchez-Pérez, J.M.; Sachmitt, D. Changes in foliar nutrient content and respiration in *Fraxinus excelsior* L., *Ulmus minor* Mill. and *Clematis vitalba* L. after prevention of floods. *Ann. For. Sci.* **1999**, *56*, 641–650. [CrossRef]
82. Mediavilla, S.; Gallardo-López, V.; González-Zurdo, P.; Escudero, A. Patterns of leaf morphology and leaf N content in relation to winter temperatures in three evergreen tree species. *Int. J. Biometeorol.* **2012**, *56*, 915–926. [CrossRef] [PubMed]
83. Lamont, B.B.; Groom, P.K.; Cowling, R.M. High leaf mass per area of related species assemblages may reflect low rainfall and carbon isotope discrimination rather than low phosphorus and nitrogen concentrations. *Funct. Ecol.* **2002**, *16*, 403–412. [CrossRef]
84. Poorter, H.; DeJong, R. Specific leaf area, chemical composition and leaf construction costs of plant species from productive and unproductive habitats. *New Phytol.* **1999**, *143*, 163–176. [CrossRef]
85. Villar, R.; Robleto, J.R.; De Jong, Y.; Poorter, H. Differences in construction costs and chemical composition between deciduous and evergreen woody species are small as compared to differences among families. *Plant Cell Environ.* **2006**, *29*, 1629–1643. [CrossRef] [PubMed]
86. Wilson, J.R.; Ludlow, M.M.; Fisher, M.J.; Schulze, E.D. Adaptation to water stress of the leaf water relations of four tropical forage species. *Aust. J. Plant Physiol.* **1980**, *7*, 207–220. [CrossRef]
87. Turner, N.C.; Begg, J.E. Plant-water relations and adaptation to stress. *Plant Soil* **1981**, *58*, 97–131. [CrossRef]
88. Morgan, J.M. Osmoregulation and water stress in higher plants. *Annu. Rev. Plant Phys.* **1984**, *35*, 299–319. [CrossRef]
89. Alvarez-Clare, S.; Kitajima, K. Physical defence traits enhance seedling survival of neotropical tree species. *Funct. Ecol.* **2007**, *21*, 1044–1054. [CrossRef]
90. Hetherington, A.M.; Woodward, F.I. The role of stomata in sensing and driving environmental change. *Nature* **2003**, *424*, 901–908. [CrossRef] [PubMed]
91. Drake, P.L.; Froend, R.H.; Franks, P.J. Smaller, faster stomata: Scaling of stomatal size, rate of response, and stomatal conductance. *J. Exp. Bot.* **2013**, *64*, 495–505. [CrossRef] [PubMed]

92. Brodribb, T. Dynamics of changing intercellular CO_2 concentration during drought and determination of minimum functional Ci. *Plant Physiol.* **2006**, *111*, 179–185. [CrossRef]
93. Savage, J.A.; Cavender-Bares, J.A. Contrasting drought survival strategies of sympatric willows (*genus: Salix*): Consequences for coexistence and habitat specialization. *Tree Physiol.* **2011**, *31*, 604–614. [CrossRef] [PubMed]